⌘ *Author's Choice*

Quantitative Proteomics: Comparison of the Macular Bruch Membrane/Choroid Complex from Age-related Macular Degeneration and Normal Eyes*[S]

Xianglin Yuan‡§, Xiaorong Gu‡§, John S. Crabb‡§, Xiuzhen Yue‡§, Karen Shadrach‡§, Joe G. Hollyfield‡§¶, and John W. Crabb‡§¶‖****

A quantitative proteomics analysis of the macular Bruch membrane/choroid complex was pursued for insights into the molecular mechanisms of age-related macular degeneration (AMD). Protein in trephine samples from the macular region of 10 early/mid-stage dry AMD, six advanced dry AMD, eight wet AMD, and 25 normal control post-mortem eyes was analyzed by LC MS/MS iTRAQ (isobaric tags for relative and absolute quantitation) technology. A total of 901 proteins was quantified, including 556 proteins from ≥3 AMD samples. Most proteins differed little in amount between AMD and control samples and therefore reflect the proteome of normal macular tissues of average age 81. A total of 56 proteins were found to be elevated and 43 were found to be reduced in AMD tissues relative to controls. Analysis by category of disease progression revealed up to 16 proteins elevated or decreased in each category. About 60% of the elevated proteins are involved in immune response and host defense, including many complement proteins and damage-associated molecular pattern proteins such as α-defensins 1–3, protein S100s, crystallins, histones, and galectin-3. Four retinoid processing proteins were elevated only in early/mid-stage AMD, supporting a role for retinoids in AMD initiation. Proteins uniquely decreased in early/mid-stage AMD implicate hematologic malfunctions and weakened extracellular matrix integrity and cellular interactions. Galectin-3, a receptor for advanced glycation end products, was the most significantly elevated protein in advanced dry AMD, supporting a role for advanced glycation end products in dry AMD progression. The results endorse inflammatory processes in both early and advanced AMD pathology, implicate different pathways of progression to advanced dry and wet AMD, and provide a new database for hypothesis-driven and discovery-based studies of AMD. ***Molecular & Cellular Proteomics 9:1031–1046, 2010.***

Age-related macular degeneration (AMD)[1] is a leading cause of blindness worldwide (1, 2) and is approaching epidemic proportions in the United States (3). AMD is a progressive disease involving multiple genetic and environmental factors. Deposition of debris (termed "drusen") along Bruch membrane in the macula is the first evidence of early AMD. Advanced AMD occurs in two forms, geographic atrophy and choroidal neovascularization (CNV). Geographic atrophy (advanced dry AMD) develops slowly and results in blindness when focal areas of the retinal pigment epithelium (RPE) degenerate in the macula. CNV (wet AMD) is characterized by the growth of new blood vessels from the choroid through Bruch membrane and the RPE. When these vessels hemorrhage, a blood clot accumulates between the RPE and the macular photoreceptors causing immediate central vision loss. CNV accounts for over 80% of debilitating visual loss in AMD, yet only 10–15% of AMD cases progress to wet AMD.

There is growing evidence that AMD is in part an age-related inflammatory disease involving complement dysregulation, including AMD susceptibility genes encoding complement factors and the presence of complement proteins in drusen (1, 2, 4). An assortment of potential inducers of AMD have been proposed; however, the causes of the disease remain poorly defined. For example, many carrying AMD risk genotypes may never develop the disease (5), and only a

From the ‡Cole Eye Institute and §Lerner Research Institute, Cleveland Clinic Foundation, Cleveland, Ohio 44195, ‖Department of Chemistry, Case Western Reserve University, Cleveland, Ohio 44106, and ¶Departments of Ophthalmology and Molecular Medicine, Cleveland Clinic Lerner College of Medicine of Case Western Reserve University, Cleveland, Ohio 44106

⌘ *Author's Choice*—Final version full access.

Received, November 4, 2009, and in revised form, January 19, 2010

Published, MCP Papers in Press, February 22, 2010, DOI 10.1074/mcp.M900523-MCP200

[1] The abbreviations used are: AMBP, alpha microglobin/bikunin precursor; AMD, age-related macular degeneration; AGE, advanced glycation end product; CEP, carboxyethylpyrrole; CNV, choroidal neovascularization; DAMP, damage-associated molecular pattern; ECM, extracellular matrix; iTRAQ, isobaric tags for relative and absolute quantitation; RPE, retinal pigment epithelium; SCX, strong cation exchange; TEAB, triethylammonium bicarbonate; PANTHER, protein analysis through evolutionary relationships; pAb, polyclonal antibody; IRBP, interphotoreceptor retinoid-binding protein; AGE-R, advanced glycation end product receptor.

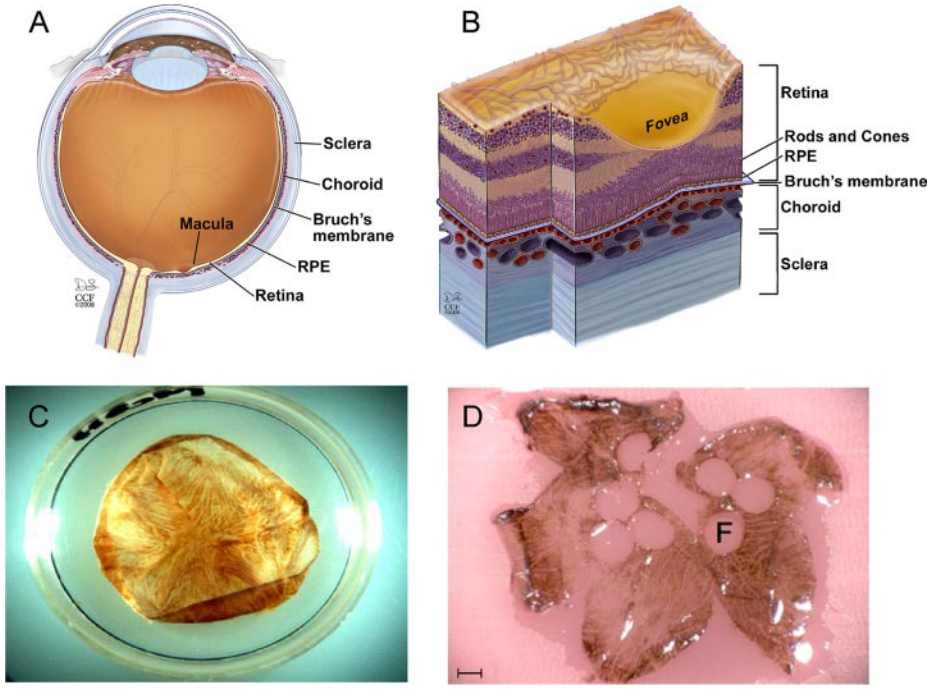

FIG. 1. **Macular Bruch membrane tissue samples.** Bruch membrane is a permeable extracellular matrix separating the RPE from the blood-bearing choroid as illustrated in a cross-section of the human eye (*A*) and a cross-section through the macular region (*B*). Photographs are shown of isolated Bruch membrane tissue before (*C*) and after (*D*) removal of 4-mm trephined tissue buttons for proteomics analysis (*F*, fovea) scale bar = 2.4 mm. *A* and *B* are reproduced with copyright permission from the Cleveland Clinic. Illustration by David Schumick. All rights reserved.

fraction of those diagnosed with early AMD progress to advanced disease (6). We have proposed that oxidative protein modifications are among the catalysts of AMD (7), and a host of elevated oxidative modifications have been reported in AMD Bruch membrane, drusen, retina, RPE, and plasma (7–14). Two of these modifications, namely carboxymethyllysine and carboxyethylpyrrole (CEP), stimulate neovascularization *in vivo* (15, 16), and immunization with CEP-adducted protein has been shown to induce a dry AMD-like phenotype in mice (17). Yet many other factors have been reported to contribute to this complex disease, including for example cigarette smoking (18), cumulative light exposure (19), lipofuscin/retinoid toxicity (20), advanced glycation end products (8–10), and microbial infection (21).

Toward a better understanding of the molecular pathways contributing to AMD pathology, we pursued quantitative proteomics analysis of the macular region of the Bruch membrane/choroid complex. Bruch membrane (see Fig. 1) is a stratified extracellular matrix (ECM) comprising a central elastin zone flanked by inner and outer collagenous layers and the basement membranes of the RPE and choriocapillaris (22). It serves as a semipermeable support for the RPE, which forms an integral part of the blood-retinal barrier and provides many vital functions for vision, including the rod retinoid visual cycle and phagocytosis of spent photoreceptors with export of degradation products to the blood. The Bruch membrane molecular sieve is thought to help regulate the diffusion of nutrients and waste products between the RPE and the bloodstream as well as to restrict cell migration (23). Age-related changes at this critical interface, including thickening and decreased permeability, have long been thought to disrupt normal retinal physiology and contribute to AMD (22, 23). We used LC MS/MS iTRAQ technology to quantify proteins from a relatively large number of age- and gender-matched AMD and normal macular tissues and to correlate proteomic changes with AMD progression. The results endorse inflammatory processes in AMD pathology, reveal molecular details previously unassociated with AMD, and provide a quantitative proteomics database from the critically important macular interface.

EXPERIMENTAL PROCEDURES

Human Bruch Membrane Tissues—Human post-mortem eyes from 24 AMD and 25 non-AMD control donors were used in this study, all between the ages of 70–87 years and including 24 males and 25 females. Normal eyes were obtained from the Cleveland Eye Bank or the National Disease Research Interchange (Philadelphia, PA). AMD donor eyes were from clinically diagnosed patients registered through the eye donor program of the Foundation Fighting Blindness (Owings Mills, MD). All post-mortem tissues complied with the policies of the Eye Bank Association of America and the Institutional Review Board of the Cleveland Clinic Foundation. The AMD disease category of donor tissues was determined by direct microscopic visualization of the macula. Eyes were enucleated between 1.5 and 7 h after death and frozen in liquid nitrogen. Tissues obtained outside of Cleveland were transferred to the laboratory on dry ice and stored at −80 °C until used. Eyes used for isolation of the Bruch membrane/choroid complex were thawed overnight at 4 °C; the anterior segment, vitreous humor, and retina were removed; the RPE was brushed away; and the choroid/Bruch membrane complex was separated from the posterior globe (7). The Bruch membrane/choroid complex was cut to lay flat, and 4–6 mm trephine tissue buttons were excised from the macular region (Fig. 1). The excised tissue buttons were gently rinsed in PBS, and then protein was extracted in 2% SDS. As post-mortem globes were acquired, three sets of AMD and control Bruch membrane/choroid samples were prepared and analyzed. Each sample is

listed in supplemental Table 1 by sample set, donor age and gender, the number and size of trephine tissue buttons, amount of protein, and whether the donor exhibited early/mid-stage AMD, advanced dry AMD, or neovascular AMD.

Sample Preparation for iTRAQ Labeling and SCX Chromatography—Bruch membrane sample sets 1 and 2 were prepared and fractionated by SCX chromatography as follows. Control and AMD tissue buttons were homogenized in 100 mM triethylammonium bicarbonate (TEAB) containing 2% SDS, and soluble protein was retrieved following centrifugation. Soluble protein was precipitated with 4 volumes of acetone to lower the SDS concentration, redissolved in 500 mM TEAB containing 0.1% SDS, and quantified by the BCA assay (Pierce) using as a reference amino acid analysis-quantified bovine serum albumin. Protein was reduced with tris(2-carboxyethyl)phosphine, cysteines were alkylated with methyl methanethiosulfonate, and the alkylated protein was digested with trypsin (24). Pooled control peptide samples were prepared as outlined in supplemental Table 1; pooled control sample 1 contained equal amounts of five non-AMD donor tissues, and pooled control sample 2 contained equal amounts of 10 non-AMD donor tissues. Tryptic peptides were labeled with iTRAQ tags (24) according to the vendor (Applied Biosystems). For sample set 1, four AMD tissues (~28–54 μg/donor) were labeled with iTRAQ tag 117 and individually mixed with an equal amount of pooled control sample 1 labeled with iTRAQ tag 115. For sample set 2, 10 AMD tissues (~45–55 μg/sample) were labeled with iTRAQ tag 117 and individually mixed with an equal amount of pooled control sample 2 labeled with iTRAQ tag 115. The iTRAQ-labeled preparations were fractionated by SCX chromatography using an Ultimate 3000 LC system (LC Packings), a PolySulfoethyl A column (1.0 × 150 mm, 5-μm particle size, 200-Å pore size), a flow rate of 50 μl/min, and a gradient of 0–600 mM KCl in 25% acetonitrile, 10 mM KH_2PO_4, pH 3. Chromatography was monitored by absorbance at 214 nm, and fractions ($n = 90$) were collected at 1-min intervals and vacuum-dried.

Sample Preparation for iTRAQ Labeling following SDS-PAGE—Bruch membrane sample set 3 was prepared and fractionated by SDS-PAGE as follows. Control and AMD tissue buttons were homogenized in 2% SDS, 62.5 mM Tris-HCl, 1 mM dithiothreitol containing 100 μl of protease inhibitor mixture (Sigma P8340) and 50 μl of phenylmethylsulfonyl fluoride/10 ml, and soluble protein was quantified by the BCA assay (Pierce). Pooled control sample 3 contained protein from 10 non-AMD donor tissues (supplemental Table 1). Each AMD sample (~50 μg) was fractionated by SDS-PAGE according to Laemmli on a gradient gel (Tris-glycine, 4–20% acrylamide, 8 cm × 8 cm × 1.5 mm, Invitrogen) adjacent to pooled control sample 3 (~50 μg), and the gel was stained with colloidal Coomassie Blue (Code Blue, Pierce). About 20–24 gel slices were excised from the top to the bottom of the lanes, and proteins were reduced with 20 mM DTT, alkylated with iodoacetamide, and digested *in situ* with trypsin (25). Tryptic peptides were extracted (26, 27), dried, redissolved in 167 mM TEAB containing 66% ethanol, and labeled with unique iTRAQ tags, using 114 or 115 tag for AMD and 116 or 117 tag for control. iTRAQ-labeled peptides from adjacent AMD and control gel bands of the same apparent mass were mixed 1:1. Excess iTRAQ reagent was removed from the peptide mixtures on the reverse phase trapping column prior to on-line LC MS/MS.

Protein Identification by On-line LC MS/MS—For on-line LC MS/MS, dried peptide fractions from SCX and SDS-PAGE were dissolved in 0.1% formic acid, 2% acetonitrile. The number of SCX fractions was reduced to 50 per sample by combining adjacent fractions exhibiting low absorbance ($\lambda = 214$ nm). In sample set 2, each SCX fraction was analyzed by both on-line LC MS/MS (~50%) and off-line LC MS/MS (~50%). On-line LC MS/MS was performed with a QTOF2 mass spectrometer (Waters) as described previously (26, 27). Protein identification utilized MASSLYNX 4.1 software (Waters), the Mascot search engine (Matrix Science, version 2.1), and the Swiss Protein sequence database (version 56.0). The Swiss Protein Database search parameters were as follows: all human entries (~20,000 total sequences), two missed tryptic cleavage sites allowed, precursor ion mass tolerance of 0.8 Da, and fragment ion mass tolerance of 0.8 Da. Fixed protein modifications included N-terminal and ε-Lys iTRAQ modifications, *S*-methyl-Cys for SCX fractions, and *S*-carboxyamidomethyl-Cys for SDS-PAGE-derived samples. Variable protein modifications included Met oxidation and ε-Lys CEP adduction. A minimum Mascot ion score of 25 was used for accepting all peptide MS/MS spectra. Two unique peptides per protein were required for all protein identifications.

Protein Identification by Off-line LC MS/MS—Off-line LC MS/MS utilized a model 4800 MALDI-TOF/TOF mass spectrometer (Applied Biosystems). SCX fractions were reduced to 40 per sample by combining low absorbance, adjacent fractions, and each was separated on a 75-μm × 15-cm PepMap100 C_{18} column (3-μm particle size, 100-Å pore size, Dionex) using an Ultimate 3000 LC system (LC Packings), aqueous trifluoroacetic acid/acetonitrile solvents, and a flow rate of ~300 nl/min with a gradient over 50 min. The eluted peptides were mixed 1:2 (v/v) with matrix (4.5 mg/ml α-cyano-4-hydroxycinnamic acid in 0.56 mM ammonium citrate) and were spotted with a Probot (LC Packings) on a MALDI target at 30-s intervals for 36 min. Collision-induced dissociation was used to generate MS/MS spectra with 1-kV collision energy. Two thousand laser shots were averaged per MS/MS spectrum, and a maximum of 20 MS/MS spectra were collected per target spot with a minimum signal-to-noise ratio of 35. Instrument operation and data acquisition utilized GPS Explorer 3.6 software (Applied Biosystems). Protein identification utilized GPS Explorer 3.6 software (Applied Biosystems), Mascot 2.1, and the Swiss Protein Database versions 51.2 and 56.0 (~20,000 total human protein sequences searched). Database searching was restricted to tryptic peptides of human sequences with two missed tryptic cleavage sites allowed, a precursor ion mass tolerance of 0.8 Da, and a fragment ion mass tolerance of 0.8 Da. Fixed modifications included N-terminal and ε-Lys iTRAQ modifications and *S*-methyl-Cys; Met oxidation was included as a variable modification. To estimate false discovery rates from QTOF2 and MALDI-TOF/TOF analyses, all peptide MS/MS spectra were searched manually (Matrix Science, version 2.2) against a randomized decoy database constructed with a script provided by Matrix Science.

Protein Quantitation—Analysis of iTRAQ labeling in QTOF2 MS/MS data was achieved with customized code written in the statistical program R (28) (available upon request). Protein quantitation required a minimum of two unique peptides per identified protein, ion intensities ≥10 for all iTRAQ tags, and Mascot peptide ion scores ≥25. All peptide and protein iTRAQ ratios were determined in natural log space and transformed to linear space for reporting. Prior to calculating protein ratios, peptide ratios from multiple charge species of the same peptide were averaged with equal weight given to each unique peptide. Protein ratios (AMD/control), S.D., and *p* values (two-sided *t* test for the null hypothesis that the peptide mean = 0 in log space) were calculated for all peptides meeting threshold criteria. For SDS-PAGE samples, at least two unique peptides meeting the threshold criteria per gel band (or adjacent gel bands) were required for quantitation. iTRAQ tags for AMD and control samples differed in mass by at least 2 daltons, therefore, no correction was needed for possible isotope overlap associated with the iTRAQ reagents. Analysis of iTRAQ labeling in MALDI-TOF/TOF MS/MS data utilized GPS Explorer 3.6 (Applied Biosystems) and required a minimum of two unique peptides per identified protein, a minimum 95% confidence interval for the Mascot protein score, and peptide Mascot ion scores ≥25. Outlier peptide ratios were eliminated using Dixon's test for proteins

TABLE I
Summary of Bruch membrane/choroid tissue samples

Tissue preparations from AMD and control donors (from supplemental Table 1) are summarized with the approximate amount of protein analyzed per donor tissue.

Property	Sample set 1		Sample set 2		Sample set 3		All samples	
	Control	AMD	Control	AMD	Control	AMD	Control	AMD
Tissue donors	5	4	10	10	10	10	25	24
Mean age (years)	80	78	82	82	81	80	81	81
Age range (years)	73–86	70–83	71–87	70–87	71–87	72–87	71–87	70–87
Male donors	1	1	5	6	6	4	12	11
Female donors	4	3	5	4	4	6	13	13
Early/mid-stage dry AMD		2		4		4		10
Advanced AMD, dry		1		3		2		6
Advanced AMD, wet (CNV)		1		3		4		8
Mean amount protein analyzed (μg)	~40	~40	~53	~53	~50	~50	~50	~50

with $n \leq 30$ peptide ions (29, 30) or for proteins with $n > 30$ peptide ions using the interquartile range function in R (28) and $k = 1.75$. Peptides assigned to more than one protein by the Mascot search program were restricted to the highest scoring protein during quantitative analysis in R. After deleting outliers and multiple copies of the same peptide, peptide ratios were normalized to the sample peptide median (*i.e.* normalized peptide ratio = unnormalized peptide ratio/median) prior to calculating mean protein ratios, S.D., and *p* values. To average results over multiple samples, protein ratios per sample were normalized to the protein median, and then average protein ratios (unadjusted), S.E., and *p* values (two-sided *t* test for the null hypothesis that the protein mean = 0 in log space) were calculated. The average data were modeled based on the protein S.E. per sample, yielding *adjusted* mean protein ratios, S.E., and *p* values over the multiple measurements.

Bioinformatics Analyses—Functional classification of proteins was performed with the protein analysis through evolutionary relationships (PANTHER) classification system (available on line). For PANTHER analysis, Swiss Protein accession numbers were converted to Reference Sequence protein accession numbers using the database for annotation, visualization and integrated discovery (DAVID). Analysis of possible pathway networks was performed with Ingenuity Pathways Analysis 8.0 (Ingenuity® Systems). Protein functional and subcellular localization analyses also utilized the Swiss Protein Database.

Western Analysis—Western blot analysis of AMD and control tissue samples was performed using 12.5% acrylamide Criterion precast gels (1 mm × 7 cm × 13.5 cm, Bio-Rad), SDS-PAGE, polyvinylidene fluoride membrane (Millipore), and chemiluminescence detection (GE Healthcare) (25). Chemiluminescence was quantified by densitometry using a Bio-Rad GS-710 instrument, and differences between control and AMD samples were evaluated using two-sided *t* tests and Excel data analysis software. Prior to Western blot analysis, sample amounts were adjusted to ~10 μg with approximately equal Coomassie Blue staining intensities. Primary antibodies included anti-α-crystallin B (rabbit polyclonal antibody (pAb), 1:1000 dilution, Assay Designs, Inc.), anti-clusterin (goat pAb, 1:5000 dilution, Chemicon International Inc.), anti-complement C3 (goat pAb, 1:1000 dilution, MP Biomedicals, LLC), anti-complement C9 (goat pAb, 1:1000 dilution, Abcam, Inc.), metalloproteinase inhibitor 3 (mouse monoclonal antibody, 1:5000 dilution, Millipore), protein-glutamine γ-glutamyltransferase 2 (goat pAb, 1:1000 dilution, Abcam Inc.), serum amyloid P (mouse monoclonal antibody, 1:250 dilution, Sigma-Aldrich), and vitronectin (rabbit pAb, 1:1000 dilution, Abcam Inc.). Secondary antibodies were obtained from GE Healthcare and Santa Cruz Biotechnology and used at 1:10,000 or 1:20,000 dilution.

RESULTS

Overview—A total of 901 proteins were quantified with two or more peptides using LC MS/MS iTRAQ technology; an additional 1543 proteins were detected with a single peptide (not shown). The samples analyzed (24 AMD and 25 control) are summarized in Table I and itemized in supplemental Table 1. The quantitative results from each sample are presented in supplemental Tables 2–35, including protein ratios, S.D., *p* values, number of unique peptides quantified, and percent sequence coverage for each protein. The results from the three sample sets were of comparable quality and appropriate for averaging based on similar distributions of protein ratios (supplemental Fig. 1), consistently low false discovery rates, and good agreement (31) between the MALDI and QTOF2 measurements (supplemental Fig. 2). Comparison of methods and the compatibility of the data sets are presented in the supplemental results and discussion.

The average relative abundance of each of the 901 proteins quantified from all 24 AMD samples is presented in supplemental Table 36. Criteria for determining whether a protein was elevated or decreased in abundance included the adjusted protein ratio and *p* value from multiple samples with only proteins quantified in ≥3 AMD samples used for comparative purposes ($n = 556$). Proteins exhibiting average protein ratios (adjusted by S.E.) above or below the group mean by at least 1 S.D. and *p* values <0.06 were considered of higher or lower abundance. The distributions of mean protein ratios for all proteins, those quantified in ≥3 AMD donor tissues, and those in ≥16 AMD samples (67% majority fraction) are shown in Fig. 2. AMD and control samples were handled identically, and the analysis of multiple samples reduced variability and improved quantitative accuracy as reflected by the S.D. values (Fig. 2). About 90% of proteins showed no significant quantitative difference between AMD and control tissues, indicating that the determined proteome largely reflects that of normal macular Bruch membrane/choroid complex.

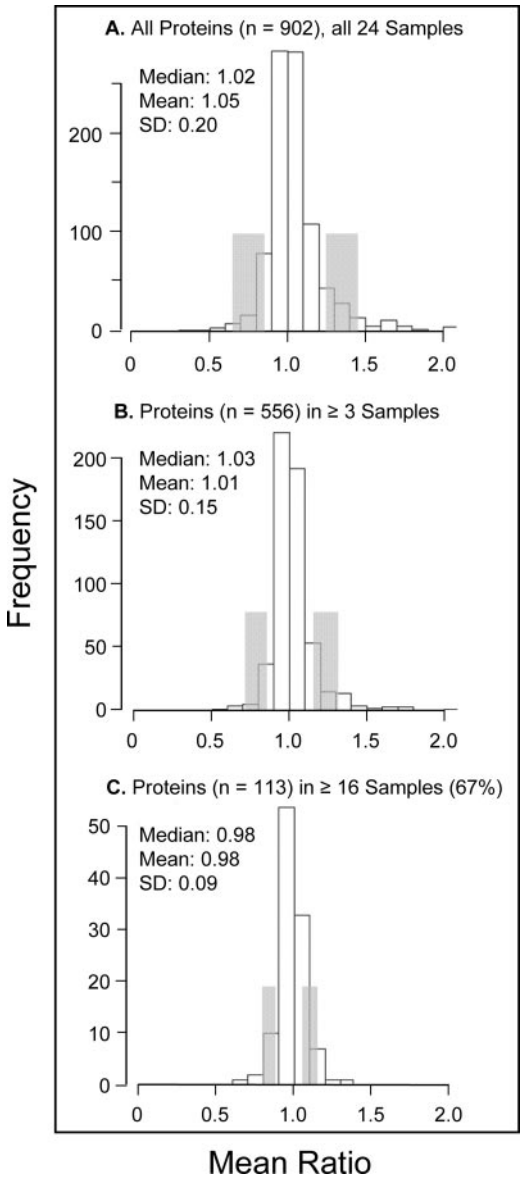

FIG. 2. **Distribution of protein ratios over all tissues.** The distributions of protein ratios (AMD/control) are shown for proteins quantified in all 24 AMD tissues analyzed, including for all proteins quantified (n = 901), proteins quantified in ≥3 tissue samples (n = 556), and proteins quantified in ≥16 samples (67% majority fraction). Median, mean, and S.D. values are indicated; protein ratios 1 S.D. from the median are *shaded*.

Proteomic Differences between AMD and Control Tissues from Comparison of All Samples—From comparison of the quantitative results from all samples, 45 proteins (~8% of those quantified in ≥3 samples) were elevated in AMD relative to control tissues (Table II), and 13 proteins (~2%) were decreased (Table III) by at least 1 S.D. from mean amounts. Western blot analysis was used to independently evaluate the abundance of eight proteins in 10 AMD and 10 control samples. The densitometric data (Fig. 3) demonstrated significant differences in the average concentrations of all eight proteins that support the iTRAQ quantitation. Immunoblots confirmed increased amounts of metalloproteinase inhibitor 3, vitronectin, C9, clusterin, α-crystallin B, protein-glutamine γ-glutamyltransferase 2, and C3 in AMD tissues and decreased amounts of serum amyloid P relative to control tissues. Further support for the iTRAQ quantitation comes from published immunohistochemistry that shows α-crystallin B, α-crystallin A (32), complement factor H and C3 (33), and metalloproteinase inhibitor 3 (34) are elevated in the AMD Bruch membrane/choroid complex. Immunohistochemical analyses have also shown several collagens, fibronectin, and laminin to be components of Bruch membrane (35), and over 25 other proteins quantified in this study have been localized to the Bruch membrane/choroid complex by immunohistochemistry (7, 36–39).

About 60% of the elevated proteins in Table II can be associated with the immune response and cellular defense processes, strongly supporting a role for inflammatory processes in AMD pathology. Complement dysregulation has been associated with AMD pathology, and many of the 16 quantified complement and complement-associated proteins were elevated in AMD tissues (Table IV), including factor H and C3 associated with AMD risk and factor B associated with AMD resistance (2, 4).

Proteomic Differences between AMD and Control Tissues by AMD Category of Progression—Average protein abundance was determined in macular tissues from 10 early/mid-stage dry AMD, six advanced dry AMD, and eight wet AMD donor eyes. Protein ratios for all proteins determined by category of AMD progression are itemized in supplemental Tables 37–39, and their distributions are shown in Fig. 4. A total of 33 proteins were found to be elevated by disease category (Table V), including 12 proteins not detected as elevated, by averaging the results from all samples (Table II). By disease category, a total of 37 proteins were found to be decreased in abundance (Table VI), including 30 not detected as reduced in the overall comparison (Table III). Supporting the capability of the methodology to detect meaningful proteomic differences, fibrinogen β was uniquely elevated in neovascular AMD, a finding consistent with the fibrovascular scar present only in wet AMD samples (supplemental Table 1). Notably, several other proteins were found to be uniquely elevated or decreased within each category of progression. Proteomic differences associated with disease progression were also sought based on protein ratio differences between categories. Proteins considered to be significantly different exhibited a mean ratio difference ≥2 S.D. from the mean difference (of the proteins compared in supplemental Tables 37–39) and a p value ≤0.06 in at least one of the categories (indicating at least one ratio significantly different from 1.0). Proteomic differences based on these criteria are summarized in Table VII for early/mid-stage dry AMD compared with wet AMD, for early/mid-stage dry AMD *versus* advanced dry AMD, and for advanced dry AMD compared with wet AMD.

TABLE II

Abundant proteins in AMD Bruch membrane/choroid

Adjusted mean protein ratios (AMD/control), S.E., *p* values, and subcellular source for abundant proteins from all 24 AMD donor tissues analyzed (from supplemental Table 36) are shown. Abundant proteins exhibited mean ratios at least 1 S.D. above the median and *p* values <0.05 (see Fig. 2). All proteins were quantified in ≥ 3 AMD donor tissues (median ratio = 1.01, S.D. = 0.15, $n = 556$). Majority fraction proteins were quantified in ≥ 16 AMD tissues ($n = 113$ proteins, median ratio = 0.98, S.D. = 0.09). Protein subcellular source is from the Swiss Protein Database: A, secreted; B, cytoplasmic; C, membrane; D, nuclear.

Swiss-Prot accession number	Subcellular source	Protein	AMD donor frequency (total = 24)	Mean protein ratio	S.E.	*p* value
Immune response and cellular defense processes						
P59666	A	Neutrophil α-defensins 1–3	7	1.77[a]	0.09	0.010
P05109	B	Protein S100-A8	12	1.71[a]	0.07	<0.001
P07360	A	Complement C8γ	7	1.66[a]	0.19	0.038
P01911	C	HLA class II histocompatibility antigen, DRB1-15β	4	1.66[a]	0.07	0.005
P13671	A	Complement C6	4	1.60[a]	0.13	0.034
P10643	A	Complement C7	8	1.58[a]	0.12	0.006
P02763	A	α_1-Acid glycoprotein 1	9	1.45[a]	0.04	<0.001
P06702	B	Protein S100-A9	12	1.44[a]	0.12	0.008
P18428	A	Lipopolysaccharide-binding protein	7	1.36[a]	0.09	0.008
P02489	B	α-Crystallin A chain	13	1.34[a]	0.08	0.003
P01903	C	HLA class II histocompatibility antigen, DRα	12	1.33[a]	0.09	0.010
P00751	A	Complement factor B	5	1.29	0.05	0.009
P01031	A	Complement C5	10	1.27	0.08	0.008
P05164	B	Myeloperoxidase	5	1.26	0.04	0.003
P06899	D	Histone H2B type 1-J	9	1.24	0.04	0.001
P08195	C	4F2 cell surface antigen heavy chain	5	1.23	0.04	0.003
P02774	A	Vitamin D-binding protein	5	1.21	0.08	0.045
P0C0L4	A	Complement C4-A	9	1.21	0.08	0.043
P04004	A	Vitronectin	24	1.21[a]	0.05	<0.001
P58876	D	Histone H2B type 1-D	5	1.20	0.05	0.020
P02748	A	Complement C9	24	1.18[a]	0.06	0.013
P08603	A	Complement factor H	6	1.17	0.04	0.008
P10909	A	Clusterin	24	1.13	0.04	0.003
P02511	B	α-Crystallin B chain	24	1.12	0.04	0.009
Q5QNW6	D	Histone H2B type 2-F	18	1.12	0.05	0.023
O75367	D	Core histone macro-H2A.1	19	1.11	0.04	0.006
P01024	A	Complement C3	22	1.10	0.04	0.022
Other regulatory processes						
P35625	A	Metalloproteinase inhibitor 3	24	1.38[a]	0.05	<0.001
P52565	B	Rho GDP-dissociation inhibitor 1	4	1.37[a]	0.08	0.016
P29762	B	Cellular retinoic acid-binding protein 1	6	1.32[a]	0.04	0.001
P30086	B	Phosphatidylethanolamine-binding protein 1	7	1.31	0.05	<0.001
P02760	A	AMBP protein	3	1.31	0.09	0.044
Q9Y277	C	Voltage-dependent anion-selective channel protein 3	8	1.19	0.06	0.023
P36955	A	Pigment epithelium-derived factor	8	1.18	0.05	0.011
Q9NQC3	C	Reticulon-4	11	1.17	0.04	0.001
P21980	B	Protein-glutamine γ-glutamyltransferase 2	23	1.11	0.03	0.002
Specialized metabolic and housekeeping processes						
P14136	B	Glial fibrillary acidic protein	4	1.78[a]	0.10	0.001
Q16518	D	Retinal pigment epithelium-specific 65-kDa protein	6	1.76[a]	0.12	0.004
Q05707	A	Collagen α1(XIV) chain	10	1.25	0.04	<0.001
P37837	B	Transaldolase	3	1.24	0.03	0.007
P02452	A	Collagen α1(I) chain	16	1.23[a]	0.06	0.003
O75874	B	Isocitrate dehydrogenase (NADP)	6	1.23	0.06	0.012
Q02978	C	2-Oxoglutarate/malate carrier protein	9	1.19	0.06	0.018
P59998	B	Actin-related protein 2/3 complex subunit 4	13	1.18	0.05	0.010
P10606	C	Cytochrome *c* oxidase subunit 5B	4	1.17	0.05	0.049

[a] Ratios at least 2 S.D. above the group median.

TABLE III
Less abundant proteins in AMD Bruch membrane/choroid

Adjusted mean protein ratios (AMD/control), S.E., *p* values, and subcellular source for less abundant proteins from all 24 AMD donor tissues analyzed (from supplemental Table 36) are shown. Less abundant proteins exhibited mean ratios at least 1 S.D. below the median and *p* values <0.06 (see Fig. 2). All proteins were quantified in ≥ 3 AMD donor tissues (median ratio = 1.01, S.D. = 0.15, $n = 556$). Majority fraction proteins were quantified in ≥ 16 AMD tissues (median ratio = 0.98, S.D. = 0.09, $n = 113$ proteins). Protein subcellular source is from the Swiss Protein Database: A, secreted; B, cytoplasmic; C, membrane; D, nuclear.

Swiss-Prot accession number	Subcellular source	Protein	AMD donor frequency (total = 24)	Mean protein ratio	S.E.	*p* value
Regulatory processes						
P21926	C	CD9 antigen	21	0.88	0.06	0.055
P22748	B	Carbonic anhydrase 4	20	0.84	0.06	0.056
P62158	B	Calmodulin	14	0.84	0.05	0.001
Q8IZP2	B	Protein FAM10A4	3	0.83	0.04	0.035
P02749	A	β_2-Glycoprotein 1	15	0.82	0.05	0.001
Q03135	C	Caveolin-1	22	0.78[a]	0.04	0.036
Q14112	A	Nidogen-2	12	0.71	0.10	0.005
Q9BXN1	A	Asporin	10	0.70[a]	0.10	0.005
Immune response and defense processes						
P04439	C	HLA class I histocompatibility antigen, A-3α	5	0.82	0.07	0.047
P02743	A	Serum amyloid P component	24	0.82	0.04	0.042
P15157	A	Tryptase α1	4	0.54[a]	0.12	0.016
Other processes						
Q9BX97	C	Plasmalemma vesicle-associated protein	3	0.72	0.07	0.040
P00403	C	Cytochrome *c* oxidase subunit 2	4	0.70[a]	0.09	0.026

[a] Ratios at least 2 S.D. below the median.

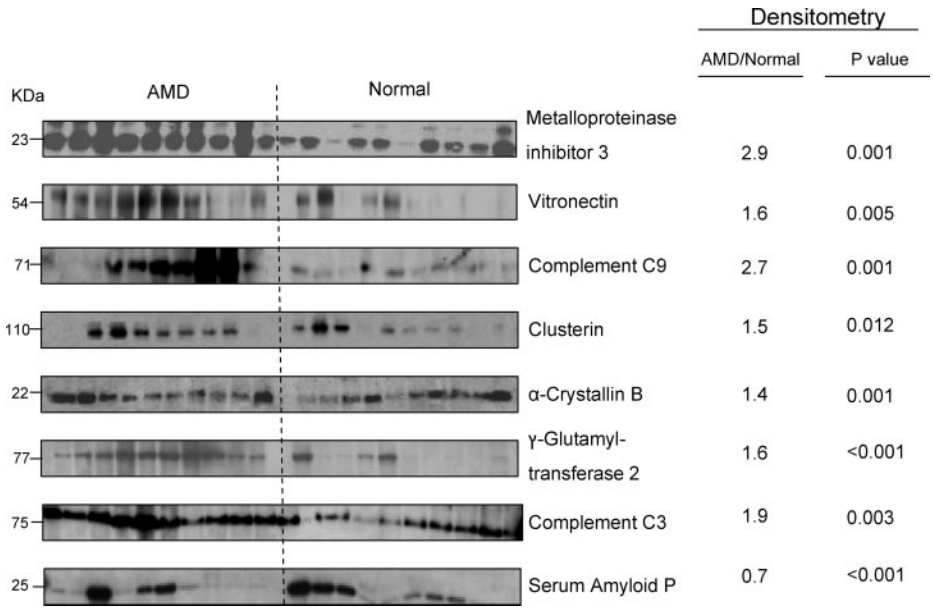

FIG. 3. **Western blot analysis.** Western blot analysis was used to evaluate the relative amounts of eight proteins in AMD and control Bruch membrane/choroid ($n = 10$ tissues each) as described under "Experimental Procedures." Average densitometry ratios (AMD/control) and *p* values (two-sided *t* test) for the indicated proteins support the protein ratios determined by LC MS/MS in Tables II and IV.

DISCUSSION

Toward a better molecular understanding of AMD, we pursued quantitative proteomics analysis of the macular Bruch membrane/choroid complex from 24 AMD and 25 control age- and gender-matched post-mortem tissue donors. AMD pathology typically involves thickening of macular Bruch membrane and decreased permeability (23) postulated to be caused by accumulation of collagen, lipids, advanced glycation end products, and RPE waste products and cross-links that trap debris within the ECM (22). Consistent with these early postulates, we detected 13 different collagens, including collagen α1(I) and collagen α1(XIV), and protein-glutamine γ-glutamyltransferase 2, a cross-linking enzyme not previously associated with AMD, that were elevated in AMD samples. More importantly, the results reveal many other changes at this critical interface and provide molecular details support-

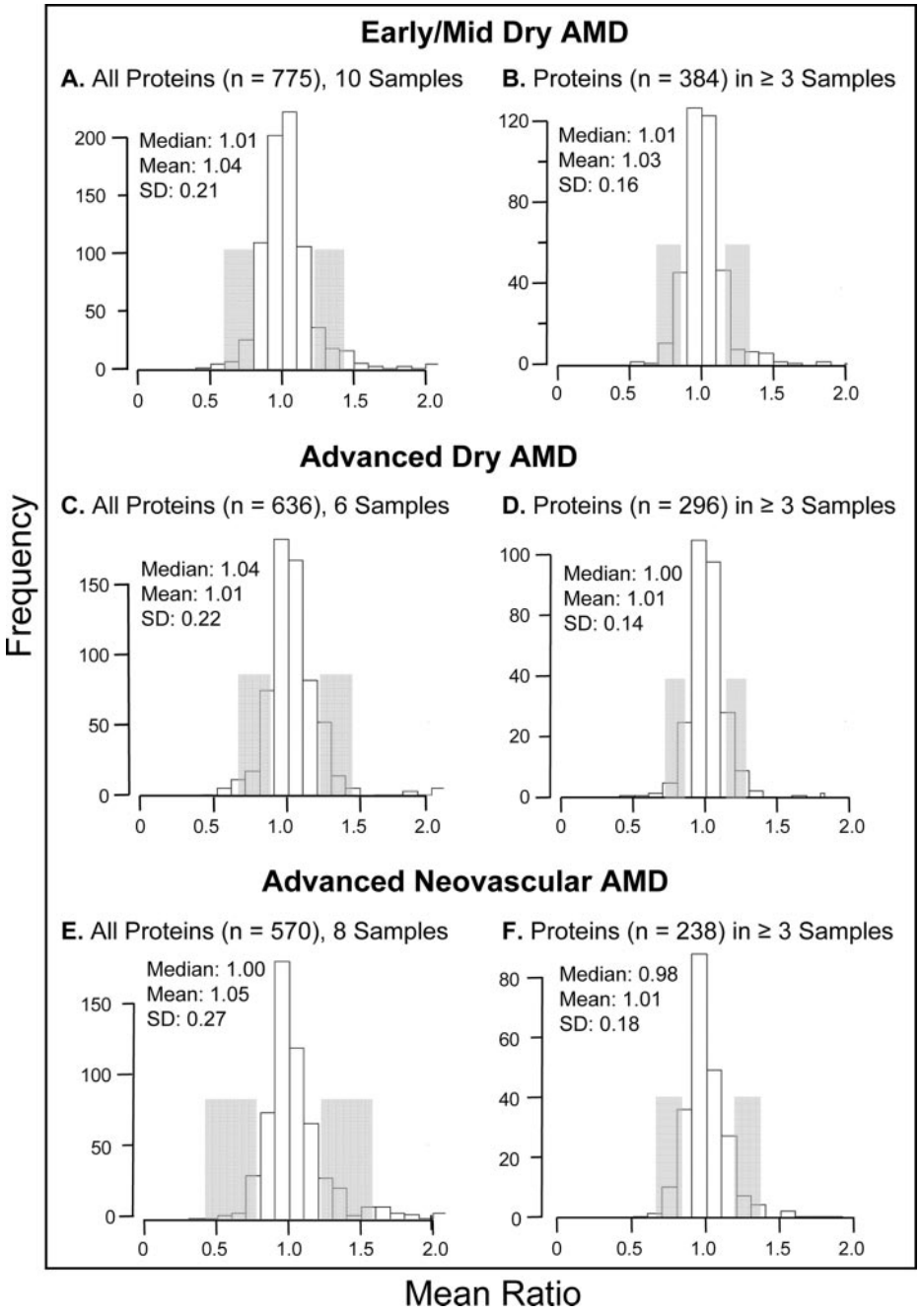

FIG. 4. **Distribution of protein ratios by disease category.** The distributions of protein ratios (AMD/control) are shown for proteins quantified in early/mid-stage AMD, advanced dry AMD, and advanced neovascular AMD tissues, including for all proteins quantified and proteins quantified in ≥3 tissues per disease category. Median, mean, and S.D. values are indicated with the number of tissues analyzed per category; protein ratios 1 S.D. from the median are *shaded*.

ing accepted as well as postulated inducers of AMD. As found for drusen (7), the quantified proteins were derived from many different cell types, including the choroid; red and white blood cell proteins; and other proteins present in the circulation. Although the retina and RPE were removed, ~15% of the quantified proteins were previously detected in human RPE (40) and in hydroquinone-induced RPE blebs (41), including 30 proteins reported to be secreted by the RPE (42). A few retina-specific proteins were detected (*e.g.* glial fibrillary acidic protein from retinal Müller cells and/or astrocytes (43)) as were ~144 unique secreted proteins. Over 80 putative exosomal proteins (44) were quantified, including for example CD9, CD63, CD81, annexins, 14-3-3 proteins, and histones, suggesting that exocytosis contributes to the identified proteome (45).

Majority of Determined Proteome Reflects That of Normal Tissues—About 90% of the 901 proteins quantified with two or more peptides (supplemental Table 36) and ~82% of the 556 proteins quantified in three or more samples were present in similar amounts in AMD and control tissues. Accordingly, the determined proteome largely reflects that of normal macular tissues from donors of average age 81. Bioinformatics

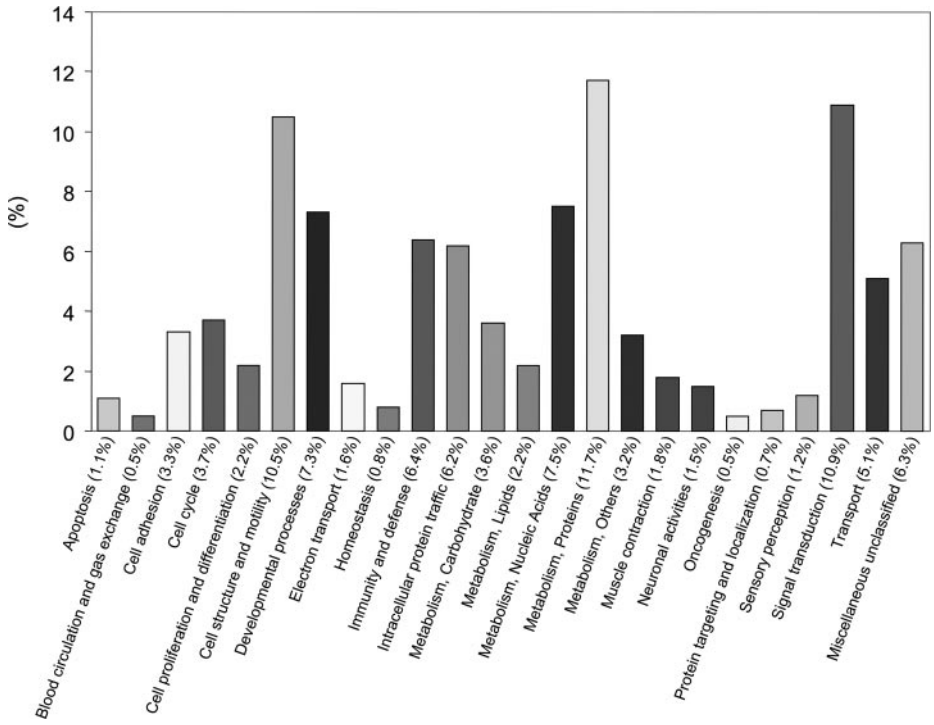

FIG. 5. **Potential functions of the Bruch membrane/choroid macular proteome.** Functional classification of the 901 proteins quantified in macular Bruch membrane/choroid was performed with the PANTHER classification system.

TABLE IV

Relative abundance of complement-associated proteins in AMD Bruch membrane/choroid

Complement-associated proteins quantified over all AMD Bruch membrane tissues are listed with adjusted mean protein ratios (AMD/control), S.E., and *p* values (from supplemental Table 36).

Swiss-Prot accession number	Protein	AMD donor frequency (total = 24)	Mean protein ratio	S.E.	*p* value
P07360	C8γ	7	1.66[a]	0.19	0.038
P13671	C6	4	1.60[a]	0.13	0.034
P10643	C7	8	1.58[a]	0.12	0.006
P00751	Complement factor B	5	1.29[a]	0.05	0.009
P01031	C5	10	1.27[a]	0.08	0.008
P0C0L4	C4-A	9	1.21[a]	0.08	0.043
P02748	C9	24	1.18[a]	0.06	0.013
P08603	Complement factor H	6	1.17[a]	0.04	0.008
P10909	Clusterin	24	1.13[a]	0.04	0.003
P01024	C3	22	1.10[a]	0.04	0.022
P07357	C8α	2	2.39	0.19	0.140
Q9BXJ0	C1q tumor necrosis factor-related protein 5	2	1.58	0.69	0.627
P07358	C8β	5	1.49	0.21	0.133
P0C0L5	C4-B	8	1.05	0.06	0.382
P00746	Complement factor D	4	1.04	0.09	0.713
P13987	CD59 (membrane attack complex inhibitor)	9	1.01	0.06	0.902

[a] Proteins significantly ($p < 0.05$) more abundant in AMD than control tissues (see Table II).

analysis using the PANTHER classification system (Fig. 5) highlights several biological processes associated with the proteome, including cellular metabolism (~28% of the 901 proteins), signal transduction (~10%), cell structure/motility (~10%), immunity and defense (~6%), and cell adhesion (~3%). Ingenuity pathway analysis of the 901 proteins implicates energy production, nucleic acid metabolism, and small molecule biochemistry as the highest scoring networks. The results suggest that the macular Bruch membrane/choroid complex performs functions similar to those of other complex ECMs in cell adhesion, tissue homeostasis, wound healing, and blood vessel growth (46, 47). The quantified proteins include ~16% secreted, ~50% cytoplasmic, ~17% membrane and membrane-associated, ~13% nuclear, and ~10% mitochondrial proteins. Secreted proteins accounted for a larger proportion of the proteins found to be elevated (~44% secreted) or decreased (~38% secreted) in AMD tissues.

TABLE V

Abundant Bruch membrane/choroid proteins by AMD category of progression

Adjusted mean protein ratios (AMD/control), S.E., and *p* values for abundant Bruch membrane proteins based on category of AMD progression are shown. Abundant proteins exhibited mean ratios at least 1 S.D. above the category median and *p* values <0.05 (from supplemental Tables 37–39 and Fig. 4). Protein subcellular source is from the Swiss Protein Database: A, secreted; B, cytoplasmic; C, membrane; D, nuclear.

Swiss-Prot accession number	Subcellular source	Protein	Donor frequency	Mean protein ratio	S.E.	*p* value
Early/mid-stage AMD (n = 10 donors)						
Only abundant in early/mid-stage AMD						
P10643	A	Complement C7	3	2.01[a]	0.13	0.032
Q16518	B	Retinal pigment epithelium-specific 65-kDa protein	4	1.86[a]	0.14	0.011
P02489	B	α-Crystallin A chain	6	1.58[a]	0.19	0.049
P02763	A	α_1-Acid glycoprotein 1	4	1.46[a]	0.03	<0.001
P01031	A	Complement C5	5	1.45[a]	0.09	0.006
P01903	C	HLA class II histocompatibility antigen, DRα chain	4	1.44[a]	0.09	0.029
Q01995	B	Transgelin	6	1.42[a]	0.10	0.012
P30086	B	Phosphatidylethanolamine-binding protein 1	3	1.41[a]	0.08	0.024
P29762	B	Cellular retinoic acid-binding protein 1	3	1.35[a]	0.03	0.009
P02511	B	α-Crystallin B chain	10	1.27	0.06	0.003
Q14103	D	Heterogeneous nuclear ribonucleoprotein D0	5	1.24	0.05	0.006
P39019	D	40 S ribosomal protein S19	4	1.21	0.06	0.021
P12271	B	Cellular retinaldehyde-binding protein 1	5	1.21	0.07	0.034
P08195	C	4F2 cell surface antigen heavy chain	4	1.20	0.04	0.008
P01011	A	α_1-Antichymotrypsin	10	1.20	0.08	0.047
Also abundant in other AMD categories						
P05109	B	Protein S100-A8	5	1.60[a]	0.08	0.001
P35625	A	Metalloproteinase inhibitor 3	10	1.38[a]	0.10	0.006
Q05707	A	Collagen α1(XIV) chain	3	1.37[a]	0.04	0.005
P02748	A	Complement C9	10	1.21	0.08	0.032
Advanced dry AMD (n = 6 donors)						
Only abundant in advanced dry AMD						
P17931	A, B, C	Galectin-3	3	1.83[a]	0.13	0.020
Q9NQC3	C	Reticulon-4	3	1.34[a]	0.07	0.016
P11166	C	Solute carrier family 2, facilitated glucose transporter	3	1.25	0.03	0.001
P06899	D	Histone H2B type 1-J	3	1.23	0.07	0.040
P62805	D	Histone H4	6	1.22	0.08	0.036
P04216	C	Thy-1 membrane glycoprotein	4	1.21	0.06	0.039
Also abundant in other AMD categories						
P06702	B	Protein S100-A9	3	1.66[a]	0.14	0.023
P35625	A	Metalloproteinase inhibitor 3	6	1.32[a]	0.10	0.021
Q05707	A	Collagen α1(XIV) chain	5	1.19	0.05	0.012
Advanced neovascular AMD (n = 8 donors)						
Only abundant in advanced neovascular AMD						
P59666	A	Neutrophil α-defensins 1–3	4	3.26[a]	0.15	0.004
P04004	A	Vitronectin	8	1.33	0.07	0.001
P02452	A	Collagen α1(I) chain	5	1.33	0.08	0.027
P02675	A	Fibrinogen β chain	3	1.28	0.08	0.028
P01024	A	Complement C3	7	1.22	0.06	0.011
Q09666	D	Neuroblast differentiation-associated protein AHNAK	4	1.19	0.03	0.002
Also abundant in other AMD categories						
P06702	B	Protein S100-A9	4	1.92[a]	0.18	0.011
P05109	B	Protein S100-A8	4	1.73[a]	0.15	0.016
P02748	A	Complement C9	8	1.51[a]	0.13	0.010
P35625	A	Metalloproteinase inhibitor 3	8	1.36	0.07	0.001

[a] Ratios at least 2 S.D. above the category median.

Proteins Elevated in AMD Relative to All Samples—Ingenuity pathway analysis of the 45 proteins found to be elevated from comparison of all AMD samples (Table II) revealed cell-mediated and humoral immune response as the highest scoring network. This network includes multiple complement proteins and damage-associated molecular patterns (DAMPs). DAMPs or alarmins are endogenous proteins released by damaged cells and are capable of binding and activating

TABLE VI

Less abundant Bruch membrane/choroid proteins by AMD category of progression

Adjusted mean protein ratios (AMD/control), S.E., and *p* values for less abundant Bruch membrane proteins based on category of AMD progression are shown. Less abundant proteins exhibited mean ratios at least 1 S.D. below the category median and *p* values <0.06 (from supplemental Tables 37–39 and Fig. 4). Protein subcellular source is from the Swiss Protein Database: A, secreted; B, cytoplasmic; C, membrane; D, nuclear.

Swiss-Prot accession number	Subcellular source	Protein	Donor frequency	Mean protein ratio	S.E.	*p* value
Early/mid-stage AMD (n = 10 donors)						
Only less abundant in early/mid-stage AMD						
P08133	B	Annexin A6	9	0.87	0.04	0.006
P51888	A	Prolargin	10	0.87	0.04	0.009
P51884	A	Lumican	9	0.85	0.05	0.009
P62158	B	Calmodulin	6	0.84	0.07	0.029
Q9BRX8	A	Uncharacterized protein C10orf58	3	0.84	0.02	0.011
P01009	A	α_1-Antitrypsin	9	0.81	0.09	0.046
P02549	B	Spectrin α chain, erythrocyte	5	0.80	0.07	0.019
P04275	A	von Willebrand factor	7	0.80	0.07	0.014
P69905	B	Hemoglobin subunit α	10	0.77	0.10	0.025
P11277	B	Spectrin β chain, erythrocyte	4	0.76	0.07	0.011
P02730	C	Band 3 anion transport protein	8	0.75	0.11	0.027
P02749	A	β_2-Glycoprotein 1	6	0.75	0.06	0.001
P02743	A	Serum amyloid P component	10	0.73	0.07	<0.001
P68871	B	Hemoglobin subunit β	10	0.71[a]	0.12	0.013
Q03135	C	Caveolin-1	9	0.70[a]	0.05	<0.001
Q14112	A	Nidogen-2	6	0.58[a]	0.12	0.007
Advanced dry AMD (n = 6 donors)						
Only less abundant in advanced dry AMD						
P68371	B	Tubulin β-2C chain	4	0.87	0.04	0.014
P62988	B, D	Ubiquitin	6	0.87	0.03	0.004
P00738	A	Haptoglobin	6	0.84	0.07	0.045
Q09666	D	Neuroblast differentiation-associated protein AHNAK	4	0.84	0.05	0.017
P31946	B	14-3-3 protein β/α	4	0.83	0.07	0.053
P23142	A	Fibulin-1	3	0.82	0.01	0.001
P80723	C	Brain acid-soluble protein 1	4	0.82	0.06	0.025
P09525	B, C	Annexin A4	4	0.80	0.06	0.037
P22748	B	Carbonic anhydrase 4	5	0.74	0.11	0.035
P43320	B	β-Crystallin B2	4	0.73[a]	0.08	0.028
Also less abundant in advanced neovascular AMD						
P10745	A	Interphotoreceptor retinoid-binding protein	5	0.45[a]	0.16	0.001
Advanced neovascular AMD (n = 8 donors)						
Only less abundant in advanced neovascular AMD						
Q02878	D	60 S ribosomal protein L6	3	0.83	0.04	0.018
P02792	B	Ferritin light chain	4	0.83	0.03	0.001
P12277	B	Creatine kinase B-type	5	0.82	0.08	0.036
P55084	C	Trifunctional enzyme subunit β, mitochondrial	4	0.82	0.04	0.016
P00338	B	L-Lactate dehydrogenase A chain	7	0.81	0.08	0.026
P04406	B	Glyceraldehyde-3-phosphate dehydrogenase	8	0.78	0.06	0.003
P14618	B	Pyruvate kinase isozymes M1/M2	7	0.78	0.04	0.000
P21926	C	CD9 antigen	7	0.78	0.11	0.056
P0C0S8	D	Histone H2A type 1	8	0.75	0.09	0.015
P10412	D	Histone H1.4	5	0.70	0.09	0.005
Also less abundant in advanced dry AMD						
P10745	A	Interphotoreceptor retinoid-binding protein	6	0.54[a]	0.08	<0.001

[a] Ratios at least 2 S.D. below the category median.

pattern recognition receptors like the complement system, toll-like receptors, and receptor for advanced glycation end products (48–50). In addition to elevated DAMPs like α-defensins 1–3, protein S100s, crystallins, and histones, several DAMPS and putative DAMPs were detected at similar levels in AMD and control samples (*e.g.* high mobility group box 1, annexins, heat shock proteins, hepatoma-derived growth factor, and nucleolin; supplemental Table 36). Other elevated proteins included the immune system modulators α_1-acidic glycoprotein 1 and vitamin D-binding protein; li-

TABLE VII

Comparison of Bruch membrane/choroid proteins by AMD category

Shown are adjusted mean protein ratios, S.E., and the ratio difference from proteins quantified in ≥3 tissues and meeting the following criteria: 1) a difference in ratios ≥2 S.D. above the mean difference and 2) at least one ratio with a *p* value ≤0.06. Subcellular localization is indicated as follows: A, secreted; B, cytoplasmic; C, membrane; D, nuclear.

Swiss Protein Accession	Subcellular Localization	Protein	Donor Frequency	Mean Protein Ratio	S.E.	*p* value	Donor Frequency	Mean Protein Ratio	S.E.	*p* value	Ratio Difference	% Ratio Difference
			Early/Mid Dry AMD Total Donors = 10				Advanced Neovascular AMD Total Donors = 8					
More Abundant in Early/Mid Stage Dry than advanced Neovascular AMD[1]												
P10745	A	Interphotoreceptor retinoid-binding protein	7	0.86	0.08	0.140	6	0.54	0.08	< 0.001	0.32	58%
P0C0S8	D	Histone H2A type 1	9	1.13	0.09	0.200	8	0.75	0.09	0.015	0.38	50%
P09972	B	Fructose-bisphosphate aldolase C	4	1.17	0.04	0.011	4	0.79	0.10	0.094	0.38	48%
P01903	C	HLA class II histocompatibility antigen, DR alpha chain	4	1.44	0.09	0.029	3	1.00	0.19	0.983	0.44	45%
P00338	B	L-lactate dehydrogenase A chain	7	1.16	0.07	0.059	7	0.81	0.08	0.026	0.35	42%
More Abundant in Advanced Neovascular than Early/Mid Stage Dry AMD[1]												
P01860	A	Ig gamma-3 chain C region	5	0.74	0.30	0.360	5	1.51	0.17	0.060	0.77	104%
P06702	B	Protein S100-A9	5	0.99	0.24	0.970	4	1.92	0.18	0.011	0.93	94%
P02675	A	Fibrinogen beta chain	5	0.88	0.14	0.360	3	1.28	0.08	0.028	0.40	45%
			Early/Mid Dry AMD Total Donors = 10				Advanced Dry AMD Total Donors = 6					
More Abundant in Early/Mid Stage Dry than Advanced Dry AMD[2]												
P10745	A	Interphotoreceptor retinoid-binding protein	7	0.86	0.08	0.111	5	0.45	0.16	0.001	0.41	93%
P43320	B	Beta-crystallin B2	6	1.23	0.20	0.340	4	0.73	0.08	0.028	0.50	67%
P10643	A	Complement C7	3	2.01	0.13	0.032	3	1.27	0.15	0.263	0.74	58%
More Abundant in Advanced Dry than Early/Mid Stage Dry AMD[2]												
P06702	B	Protein S100-A9	5	0.99	0.24	0.970	3	1.66	0.14	0.023	0.67	68%
P17931	ABD	Galectin-3	5	1.09	0.09	0.390	3	1.83	0.13	0.020	0.74	67%
P01871	AC	Ig mu chain C region	6	0.82	0.14	0.210	4	1.30	0.11	0.058	0.48	58%
P02549	B	Spectrin alpha chain, erythrocyte	5	0.80	0.07	0.019	3	1.16	0.13	0.300	0.36	45%
P11277	B	Spectrin beta chain, erythrocyte	4	0.76	0.07	0.011	3	1.11	0.05	0.112	0.35	45%
			Advanced Dry AMD Total Donors = 6				Advanced Neovascular AMD Total Donors = 8					
More Abundant in Advanced Dry than Advanced Neovascular AMD[3]												
P17931	ABD	Galectin-3	3	1.83	0.13	0.020	4	0.95	0.07	0.464	0.88	92%
P0C0S8	D	Histone H2A type 1	5	1.32	0.23	0.301	8	0.75	0.09	0.015	0.56	75%
P11166	C	Solute carrier family 2, facilitated glucose transporter	3	1.25	0.03	0.001	3	0.87	0.17	0.436	0.38	44%
More Abundant in Advanced Neovascular than Advanced Dry AMD[3]												
P59666	A	Neutrophil alpha defensin 1~3	3	0.94	0.44	0.901	4	3.26	0.15	0.004	2.32	247%
P02748	AC	Complement C9	6	0.99	0.09	0.888	8	1.51	0.13	0.010	0.53	53%
P09525	BC	Annexin A4	4	0.80	0.06	0.037	4	1.16	0.04	0.021	0.35	44%
Q09666	D	Neuroblast differentiation-associated protein AHNAK	4	0.84	0.05	0.017	4	1.19	0.03	0.002	0.35	42%

[1] From 231 proteins compared in supplemental Table 37.
[2] From 280 proteins compared in supplemental Table 38.
[3] From 204 proteins compared in supplemental Table 39.

popolysaccharide-binding protein; an acute phase response protein, myeloperoxidase, of the defense system of polymorphonuclear leukocytes; and vitronectin or serum spreading factor, a protein with cell adhesion and complement inhibition functions.

About 40% of the elevated proteins in Table II function in a variety of other biological processes. Elevated regulatory proteins previously detected in drusen (7) include metalloproteinase inhibitor 3; AMBP, a protease inhibitor; and pigment epithelium-derived factor, a neurotrophic antiangiogenic protein. Other regulatory proteins not previously associated with AMD include phosphatidylethanolamine-binding protein 1, a lipid-binding serine protease inhibitor; Rho GDP-dissociation inhibitor 1, whose overexpression can disrupt cell adhesion; reticulon-4, a neurite growth inhibitor and regulator of cell migration; cellular retinoic acid-binding protein, a retinoid transport protein; and voltage-dependent anion-selective channel protein 3, a diffusion regulator of small molecules. Ingenuity pathway analysis assigned these proteins to a network involving cell survival and hematologic processes.

Several other proteins with specialized metabolic or housekeeping functions were elevated as shown in Table II. For example, RPE65, an isomerase that produces 11-*cis*-retinol in the RPE, was significantly elevated as was glial fibrillary acidic protein, an intermediate filament protein upregulated by retinal Müller cells and astrocytes during gliosis. Elevated housekeeping proteins include actin-related protein 2/3 complex subunit 4, transaldolase, and isocitrate dehydrogenase. Mitochondrial dysfunction has been proposed to contribute to aging (51) and AMD pathology (52), and mitochondrial cytochrome *c* oxidase subunit 5B and 2-oxoglutarate/malate carrier protein were found to be elevated.

Proteins Elevated in Early/Mid-stage AMD—Of potential significance to disease initiation, 19 proteins were elevated in early/mid-stage AMD tissues, including 12 proteins elevated ≥2 S.D. (Table V). Fifteen of these proteins were uniquely elevated, eight of which are associated with inflammatory processes and cellular defense, namely C5, C7, α_1-acid glycoprotein 1, α_1-antichymotrypsin, α-crystallin A, α-crystallin B, HLA class II histocompatability antigen

DRα, and 4F2 cell surface antigen heavy chain. In addition, HLA class II histocompatibility antigen DRα and C7 were more abundant in early/mid-stage AMD than in advanced dry or wet AMD (Table VII). These findings support the role of inflammatory processes in initiating events of AMD.

Interestingly, four retinoid processing proteins were detected at elevated levels in early/mid-stage AMD (Table V and VII), namely RPE65, cellular retinoic acid-binding protein 1, cellular retinaldehyde-binding protein, and interphotoreceptor retinoid-binding protein (IRBP). Cellular retinoic acid-binding protein 1 is a transporter of oxidized vitamin A, and RPE65 and cellular retinaldehyde-binding protein function in the RPE production of 11-*cis*-retinal for visual pigment regeneration. The function of IRBP remains poorly defined, but it binds multiple hydrophobic ligands and may be involved in scavenging oxidatively damaged retinoids and fatty acids (53). Elevated retinoid processing proteins may reflect increased RPE synthesis of these proteins to compensate for increased oxidative damage to retinoids. Retinoids are highly susceptible to oxidation and can be toxic to cells, and their by-products accumulate in RPE lipofuscin granules (27) with age and in AMD and can activate complement (54). Elevated retinoid processing proteins in early/mid-stage AMD add support to the thesis that retinoids play a role in AMD pathology (20). This hypothesis, supported recently by a study showing an AMD-like phenotype in mice unable to clear all-*trans*-retinal from the photoreceptors (55), has led to a clinical trial testing the efficacy of a potential AMD therapeutic that inhibits the production of retinoids in the eye (56).

Proteins Elevated in Advanced Dry AMD—Nine proteins were elevated in advanced dry AMD samples, including six that were uniquely elevated and four elevated $\geq$2 S.D. (Table V). Galectin-3, also known as advanced glycation end product receptor 3 (AGE-R3) (57), was the most significantly elevated (up over 80%) in advanced dry AMD samples (Tables V and VII). Previous studies have associated elevated AGE receptors, namely RAGE and AGE-R1, with dry AMD (10, 58); demonstrated increased pentosidine, a cross-linking AGE, in Bruch membrane with increasing age (59); and shown that pentosidine and carboxymethyllysine are elevated in the systemic circulation in AMD (14). The present results support a role for AGEs and receptors for AGEs in the progression to advanced dry AMD. In contrast to wet AMD, we found no complement proteins elevated in advanced dry AMD tissues, but histone H2B type 1-J and histone H4 were uniquely elevated, perhaps as components of so-called "neutrophil extracellular traps" (50) formed during cell death processes (49). A majority ($\sim$67%) of the proteins elevated in advanced dry AMD were different from those elevated in neovascular AMD, implicating significantly different mechanisms of progression.

Proteins Elevated in Neovascular AMD—Ten proteins were found to be elevated in wet AMD macular tissues, including six that were uniquely elevated and four elevated $\geq$2 S.D. (Table V). Five uniquely elevated proteins were secreted with neutrophil α-defensins 1–3 being the most abundant in CNV samples (up over 200%). This peptide functions in innate and adaptive immunity, including for example, recruitment of T cells and immature dendritic cells, stimulation of the production of inflammatory mediators and regulation of complement activation. Notably, α-defensins 1–3 were significantly elevated in CNV tissues relative to advanced dry AMD (Table VII) and may have utility as an AMD biomarker for susceptibility to CNV. Vitronectin, a complement pathway inhibitor; C3; and neuroblast differentiation-associated protein AHNAK were all uniquely elevated in the CNV tissues and may also offer potential as AMD biomarkers of progression. IgG was more abundant in wet AMD than early dry AMD tissues (Table VII), suggesting that antibody deposition may contribute to progression to wet AMD. Elevated metalloproteinase inhibitor 3 and S110-A9 were common to both forms of advanced AMD; however, the majority ($\sim$80%) of the proteins found to be elevated in neovascular AMD were different from those elevated in advanced dry AMD.

Proteins Decreased in AMD—Whether decreased protein abundance in AMD reflects consequences or possible causes of AMD remains to be determined, but identifying the pathways associated with such proteins should enhance molecular understanding of this complex disease. From comparison of all 24 AMD samples, a small fraction of the quantified proteins ($<$2%) were significantly reduced in AMD (Table III). Asporin, nidogen-2, and caveolin-1 were decreased more than others (down 22–30%) in the greatest number of samples. Over half of the decreased proteins can be associated with cell adhesion and protein interactions (asporin, nidogen-2, protein FAM10A4, and CD9) or vascularization and angiogenesis (tryptase α1, plasmalemma vesicle-associated protein, caveolin-1, and β_2-glycoprotein 1). The highest scoring Ingenuity Pathway networks for the 13 decreased proteins in Table III concerned cell-to-cell signaling/interaction, cell death, and hematological system development/function.

From early/mid-stage AMD macular samples, 16 proteins were found to be uniquely decreased (Table VI), including five erythrocyte-specific proteins (hemoglobins α and β, spectrins α and β, and band 3 anion transport protein), implicating hematological malfunction. Several secreted collagen-binding proteins were reduced in early/mid-stage AMD (prolargin, lumican, von Willebrand factor, and nidogen-2 (the most significantly reduced, $\sim$42%)), implicating weakened structural integrity and/or disrupted cellular interactions. Other reduced proteins in early/mid-stage AMD suggest altered signal transduction and cellular regulation (calmodulin, β_2-glycoprotein 1, serum amyloid P, caveolin-1, annexin A6, and α_1-antitypsin). Ingenuity pathway analysis assigned cellular growth/proliferation, hematological disease, and cell morphology as the

highest scoring networks involving the 16 proteins decreased in early/mid-stage AMD.

Ten proteins were found to be uniquely decreased from analysis of advanced dry AMD macular samples (Table VI). IRBP (also decreased in wet AMD), β-crystallin B2, and carbonic anhydrase 4 were reduced the most (~26–55%) in four to five samples. Ubiquitin, a protein modifier with multiple signaling functions, and haptoglobin, which functions in iron homeostasis and hemoglobin turnover, were reduced in all advanced dry AMD samples. Interestingly, neuroblast differentiation-associated AHNAK, a membrane remodeling and repair protein, was reduced in geographic atrophy but elevated in neovascular AMD samples. Ingenuity pathway analysis assigned cellular compromise, drug metabolism, and molecular transport as the highest scoring networks involving the 11 proteins decreased in geographic atrophy.

From wet AMD macular samples, 10 proteins were found to be uniquely reduced (Table VI). Two histones, CD9, and three glycolytic enzymes were reduced ~22–30% in five to eight samples; however, IRBP (also decreased in geographic atrophy) was the most significantly reduced (≥2 S.D.). Most of these changes can be associated with cell death. Also decreased in CNV samples were mitochondrial trifunctional enzyme β, creatine kinase B, and ferritin light chain. Ingenuity pathway analysis assigned the highest scoring networks involving the 11 proteins decreased in wet AMD to cell cycle, tissue development, and cellular development.

Conclusions—A database of 901 quantified proteins has been established from the macular Bruch membrane/choroid complex of AMD and normal donors. The majority of these proteins differed little in amount between AMD and controls, and bioinformatics analyses suggest that they perform a host of biological processes in support of the health of the retina. From comparison of all AMD samples together as well as by comparison of samples by category of disease progression, 56 proteins were found to be elevated and 43 proteins to be reduced in AMD tissues. Complement proteins, DAMPs, and other immune response and host defense proteins were the most common elevated components, strongly endorsing inflammatory processes in both initiating events and advanced AMD. Four retinoid processing proteins found to be uniquely elevated in early/mid-stage AMD add support to the thesis that retinoids (and lipofuscin) play a role in AMD initiation. Galectin-3 (AGE-R3) was found to be elevated uniquely in advanced dry AMD, adding support to the thesis that AGEs and receptors for AGEs contribute to AMD. Proteins uniquely decreased in early/mid-stage AMD suggest hematologic malfunctions, weakened ECM structural integrity, and disrupted ECM cellular interactions. Different proteins were elevated or deceased in advanced dry *versus* wet AMD, indicating substantially different mechanisms of disease progression. Uniquely elevated proteins such as galectin-3 in advanced dry AMD and α-defensins 1–3 in neovascular AMD may not only contribute to disease progression, but these and others may be useful as AMD biomarkers. This quantitative proteomics database provides a new foundation for hypothesis-driven studies probing AMD mechanisms as well as for discovery-based efforts to develop proteomic and genomic prognostic signatures of AMD.

Acknowledgment—We are grateful to James Bena, Cleveland Clinic Foundation Quantitative Health Sciences, for assistance with statistical analyses.

* This work was supported, in whole or in part, by National Institutes of Health Grants EY14239, EY14240, and EY15638. This work was also supported by Ohio Biomedical Research Technology Transfer Grant 05-29, a research center grant from The Foundation Fighting Blindness, the Llura and Gordon Gund Foundation, a challenge grant from Research to Prevent Blindness (RPB), an RPB senior investigator award (to J. W. C.), a Steinbach award (to J. W. C.), Genentech, and The Cleveland Clinic Foundation.

S This article contains supplemental results and discussion, Tables 1–39, and Figs. 1 and 2.

** To whom correspondence should be addressed: Cole Eye Inst., Cleveland Clinic Foundation (i-31), 9500 Euclid Ave., Cleveland, OH 44195. Tel.: 216-445-0425; Fax: 216-445-3670; E-mail: Crabbj@ccf.org.

REFERENCES

1. Jager, R. D., Mieler, W. F., and Miller, J. W. (2008) Age-related macular degeneration. *N. Engl. J. Med.* **358,** 2606–2617
2. Ding, X., Patel, M., and Chan, C. C. (2009) Molecular pathology of age-related macular degeneration. *Prog. Retin. Eye Res.* **28,** 1–18
3. Friedman, D. S., O'Colmain, B. J., Muñoz, B., Tomany, S. C., McCarty, C., de Jong, P. T., Nemesure, B., Mitchell, P., and Kempen, J. (2004) Prevalence of age-related macular degeneration in the United States. *Arch. Ophthalmol.* **122,** 564–572
4. Anderson, D. H., Radeke, M. J., Gallo, N. B., Chapin, E. A., Johnson, P. T., Curletti, C. R., Hancox, L. S., Hu, J., Ebright, J. N., Malek, G., Hauser, M. A., Rickman, C. B., Bok, D., Hageman, G. S., and Johnson, L. V. (2010) The pivotal role of the complement system in aging and age-related macular degeneration: hypothesis re-visited. *Prog. Retin. Eye Res.* **29,** 95–112
5. Fritsche, L. G., Loenhardt, T., Janssen, A., Fisher, S. A., Rivera, A., Keilhauer, C. N., and Weber, B. H. (2008) Age-related macular degeneration is associated with an unstable ARMS2 (LOC387715) mRNA. *Nat. Genet.* **40,** 892–896
6. Age Related Eye Disease Study Group (2001) A randomized, placebo-controlled, clinical trial of high-dose supplementation with vitamins C and E, beta carotene, and zinc for age-related macular degeneration and vision loss. *Arch. Ophthalmol.* **119,** 1417–1436
7. Crabb, J. W., Miyagi, M., Gu, X., Shadrach, K., West, K. A., Sakaguchi, H., Kamei, M., Hasan, A., Yan, L., Rayborn, M. E., Salomon, R. G., and Hollyfield, J. G. (2002) Drusen proteome analysis: an approach to the etiology of age-related macular degeneration. *Proc. Natl. Acad. Sci. U.S.A.* **99,** 14682–14687
8. Ishibashi, T., Murata, T., Hangai, M., Nagai, R., Horiuchi, S., Lopez, P. F., Hinton, D. R., and Ryan, S. J. (1998) Advanced glycation end products in age-related macular degeneration. *Arch. Ophthalmol.* **116,** 1629–1632
9. Hammes, H. P., Hoerauf, H., Alt, A., Schleicher, E., Clausen, J. T., Bretzel, R. G., and Laqua, H. (1999) N(epsilon)(carboxymethyl)lysin and the AGE receptor RAGE colocalize in age-related macular degeneration. *Invest. Ophthalmol. Vis. Sci.* **40,** 1855–1859
10. Howes, K. A., Liu, Y., Dunaief, J. L., Milam, A., Frederick, J. M., Marks, A., and Baehr, W. (2004) Receptor for advanced glycation end products and age-related macular degeneration. *Invest. Ophthalmol. Vis. Sci.* **45,** 3713–3720
11. Shen, J. K., Dong, A., Hackett, S. F., Bell, W. R., Green, W. R., and Campochiaro, P. A. (2007) Oxidative damage in age-related macular

degeneration. *Histol. Histopathol.* **22,** 1301–1308
12. Gu, X., Meer, S. G., Miyagi, M., Rayborn, M. E., Hollyfield, J. G., Crabb, J. W., and Salomon, R. G. (2003) Carboxyethylpyrrole protein adducts and autoantibodies, biomarkers for age-related macular degeneration. *J. Biol. Chem.* **278,** 42027–42035
13. Gu, J., Pauer, G. J., Yue, X., Narendra, U., Sturgill, G. M., Bena, J., Gu, X., Peachey, N. S., Salomon, R. G., Hagstrom, S. A., and Crabb, J. W. (2009) Assessing susceptibility to age-related macular degeneration with proteomic and genomic biomarkers. *Mol. Cell. Proteomics* **8,** 1338–1349
14. Ni, J., Yuan, X., Gu, J., Yue, X., Gu, X., Nagaraj, R. H., and Crabb, J. W. (2009) Plasma protein pentosidine and carboxymethyllysine, biomarkers for age-related macular degeneration. *Mol. Cell. Proteomics* **8,** 1921–1933
15. Okamoto, T., Tanaka, S., Stan, A. C., Koike, T., Kase, M., Makita, Z., Sawa, H., and Nagashima, K. (2002) Advanced glycation end products induce angiogenesis in vivo. *Microvasc. Res.* **63,** 186–195
16. Ebrahem, Q., Renganathan, K., Sears, J., Vasanji, A., Gu, X., Lu, L., Salomon, R. G., Crabb, J. W., and Anand-Apte, B. (2006) Carboxyethylpyrrole oxidative protein modifications stimulate neovascularization: Implications for age-related macular degeneration. *Proc. Natl. Acad. Sci. U.S.A.* **103,** 13480–13484
17. Hollyfield, J. G., Bonilha, V. L., Rayborn, M. E., Yang, X., Shadrach, K. G., Lu, L., Ufret, R. L., Salomon, R. G., and Perez, V. L. (2008) Oxidative damage-induced inflammation initiates age-related macular degeneration. *Nat. Med.* **14,** 194–198
18. Seddon, J. M., Willett, W. C., Speizer, F. E., and Hankinson, S. E. (1996) A prospective study of cigarette smoking and age-related macular degeneration in women. *JAMA* **276,** 1141–1146
19. Cruickshanks, K. J., Klein, R., Klein, B. E., and Nondahl, D. M. (2001) Sunlight and the 5-year incidence of early age-related maculopathy: the beaver dam eye study. *Arch. Ophthalmol.* **119,** 246–250
20. Sparrow, J. R., and Boulton, M. (2005) RPE lipofuscin and its role in retinal pathobiology. *Exp. Eye Res.* **80,** 595–606
21. Shen, D., Tuo, J., Patel, M., Herzlich, A. A., Ding, X., Chew, E. Y., and Chan, C. C. (2009) Chlamydia pneumoniae infection, complement factor H variants and age-related macular degeneration. *Br. J. Ophthalmol.* **93,** 405–408
22. Booij, J. C., Baas, D. C., Beisekeeva, J., Gorgels, T. G., and Bergen, A. A. (2010) The dynamic nature of Bruch's membrane. *Prog. Retin. Eye Res.* **29,** 1–18
23. Goldberg, M. F. (1976) Editorial: Bruch's membrane and vascular growth. *Invest. Ophthalmol.* **15,** 443–446
24. Ross, P. L., Huang, Y. N., Marchese, J. N., Williamson, B., Parker, K., Hattan, S., Khainovski, N., Pillai, S., Dey, S., Daniels, S., Purkayastha, S., Juhasz, P., Martin, S., Bartlet-Jones, M., He, F., Jacobson, A., and Pappin, D. J. (2004) Multiplexed protein quantitation in Saccharomyces cerevisiae using amine-reactive isobaric tagging reagents. *Mol. Cell. Proteomics* **3,** 1154–1169
25. Miyagi, M., Sakaguchi, H., Darrow, R. M., Yan, L., West, K. A., Aulak, K. S., Stuehr, D. J., Hollyfield, J. G., Organisciak, D. T., and Crabb, J. W. (2002) Evidence that light modulates protein nitration in rat retina. *Mol. Cell. Proteomics* **1,** 293–303
26. Zhan, X., Du, Y., Crabb, J. S., Gu, X., Kern, T. S., and Crabb, J. W. (2008) Targets of tyrosine nitration in diabetic rat retina. *Mol. Cell. Proteomics* **7,** 864–874
27. Ng, K. P., Gugiu, B., Renganathan, K., Davies, M. W., Gu, X., Crabb, J. S., Kim, S. R., Rózanowska, M. B., Bonilha, V. L., Rayborn, M. E., Salomon, R. G., Sparrow, J. R., Boulton, M. E., Hollyfield, J. G., and Crabb, J. W. (2008) Retinal pigment epithelium lipofuscin proteomics. *Mol. Cell. Proteomics* **7,** 1397–1405
28. R Development Team (2008) *R: a Language and Environment for Statistical Computing*, R Foundation for Statistical Computing, Vienna, Austria
29. Dixon, W. M. (1953) Processing data for outliers. *Biometrics* **9,** 74–89
30. Rorabacher, D. B. (1991) Statistical treatment for rejection of deviant values: critical values of Dixon's "Q" parameter and related subrange ratios at the 95% confidence interval. *Anal. Chem.* **63,** 139–146
31. Bland, J. M., and Altman, D. G. (1986) Statistical methods for assessing agreement between two methods of clinical measurement. *Lancet* **1,** 307–310
32. Nakata, K., Crabb, J. W., and Hollyfield, J. G. (2005) Crystallin distribution in Bruch's membrane-choroid complex from AMD and age-matched donor eyes. *Exp. Eye Res.* **80,** 821–826
33. Hageman, G. S., Anderson, D. H., Johnson, L. V., Hancox, L. S., Taiber, A. J., Hardisty, L. I., Hageman, J. L., Stockman, H. A., Borchardt, J. D., Gehrs, K. M., Smith, R. J., Silvestri, G., Russell, S. R., Klaver, C. C., Barbazetto, I., Chang, S., Yannuzzi, L. A., Barile, G. R., Merriam, J. C., Smith, R. T., Olsh, A. K., Bergeron, J., Zernant, J., Merriam, J. E., Gold, B., Dean, M., and Allikmets, R. (2005) A common haplotype in the complement regulatory gene factor H (HF1/CFH) predisposes individuals to age-related macular degeneration. *Proc. Natl. Acad. Sci. U.S.A.* **102,** 7227–7232
34. Kamei, M., and Hollyfield, J. G. (1999) TIMP-3 in Bruch's membrane: changes during aging and in age-related macular degeneration. *Invest. Ophthalmol. Vis. Sci.* **40,** 2367–2375
35. Marshall, J., Hussain, A. A., Starite, C., Moore, D. J., and Patmore, A. L. (1998) Aging and Bruch's membrane, in *The Retinal Pigment Epithelium* (Marmor, M. F., and Wolfensberger, T. J., eds) pp. 669–692, Oxford University Press, New York
36. Mullins, R. F., Russell, S. R., Anderson, D. H., and Hageman, G. S. (2000) Drusen associated with aging and age-related macular degeneration contain proteins common to extracellular deposits associated with atherosclerosis, elastosis, amyloidosis, and dense deposit disease. *FASEB J.* **14,** 835–846
37. Sakaguchi, H., Miyagi, M., Shadrach, K. G., Rayborn, M. E., Crabb, J. W., and Hollyfield, J. G. (2002) Clusterin is present in drusen in age-related macular degeneration. *Exp. Eye Res.* **74,** 547–549
38. Russell, S. R., Mullins, R. F., Schneider, B. L., and Hageman, G. S. (2000) Location, substructure, and composition of basal laminar drusen compared with drusen associated with aging and age-related macular degeneration. *Am. J. Ophthalmol.* **129,** 205–214
39. Gold, B., Merriam, J. E., Zernant, J., Hancox, L. S., Taiber, A. J., Gehrs, K., Cramer, K., Neel, J., Bergeron, J., Barile, G. R., Smith, R. T., Hageman, G. S., Dean, M., and Allikmets, R. (2006) Variation in factor B (BF) and complement component 2 (C2) genes is associated with age-related macular degeneration. *Nat. Genet.* **38,** 458–462
40. West, K. A., Yan, L., Shadrach, K., Sun, J., Hasan, A., Miyagi, M., Crabb, J. S., Hollyfield, J. G., Marmorstein, A. D., and Crabb, J. W. (2003) Protein database, human retinal pigment epithelium. *Mol. Cell. Proteomics* **2,** 37–49
41. Alcazar, O., Hawkridge, A. M., Collier, T. S., Cousins, S. W., Bhattacharya, S. K., Muddiman, D. C., and Marin-Castano, M. E. (2009) Proteomics characterization of cell membrane blebs in human retinal pigment epithelium cells. *Mol. Cell. Proteomics* **8,** 2201–2211
42. An, E., Lu, X., Flippin, J., Devaney, J. M., Halligan, B., Hoffman, E. P., Strunnikova, N., Csaky, K., and Hathout, Y. (2006) Secreted proteome profiling in human RPE cell cultures derived from donors with age related macular degeneration and age matched healthy donors. *J. Proteome Res.* **5,** 2599–2610
43. Sarthy, V. P., Brodjian, S. J., Dutt, K., Kennedy, B. N., French, R. P., and Crabb, J. W. (1998) Establishment and characterization of a retinal Muller cell line. *Invest. Ophthalmol. Vis. Sci.* **39,** 212–216
44. Oliver, C., and Vidal, M. (2007) Proteomic analysis of secreted exosomes, in *Subcellular Proteomics* (Bertrand, E., and Faupel, M., eds) pp. 99–131, Springer, New York
45. Wang, A. L., Lukas, T. J., Yuan, M., Du, N., Tso, M. O., and Neufeld, A. H. (2009) Autophagy and exosomes in the aged retinal pigment epithelium: possible relevance to drusen formation and age-related macular degeneration. *PLoS One* **4,** e4160
46. Berrier, A. L., and Yamada, K. M. (2007) Cell-matrix adhesion. *J. Cell. Physiol.* **213,** 565–573
47. Cheresh, D. A., and Stupack, D. G. (2008) Regulation of angiogenesis: apoptotic cues from the ECM. *Oncogene* **27,** 6285–6298
48. Lotze, M. T., Zeh, H. J., Rubartelli, A., Sparvero, L. J., Amoscato, A. A., Washburn, N. R., Devera, M. E., Liang, X., Tör, M., and Billiar, T. (2007) The grateful dead: damage-associated molecular pattern molecules and reduction/oxidation regulate immunity. *Immunol. Rev.* **220,** 60–81
49. Pisetsky, D. S. (2007) The role of nuclear macromolecules in innate immunity. *Proc. Am. Thorac. Soc.* **4,** 258–262
50. Urban, C. F., Ermert, D., Schmid, M., Abu-Abed, U., Goosmann, C., Nacken, W., Brinkmann, V., Jungblut, P. R., and Zychlinsky, A. (2009) Neutrophil extracellular traps contain calprotectin, a cytosolic protein

complex involved in host defense against Candida albicans. *PLoS Pathog.* **5,** e1000639
51. Knott, A. B., Perkins, G., Schwarzenbacher, R., and Bossy-Wetzel, E. (2008) Mitochondrial fragmentation in neurodegeneration. *Nat. Rev. Neurosci.* **9,** 505–518
52. Nordgaard, C. L., Karunadharma, P. P., Feng, X., Olsen, T. W., and Ferrington, D. A. (2008) Mitochondrial proteomics of the retinal pigment epithelium at progressive stages of age-related macular degeneration. *Invest. Ophthalmol. Vis. Sci.* **49,** 2848–2855
53. Saari, J. C., and Crabb, J. W. (2008) Genetic and proteomic analyses of the mouse visual cycle, in *Eye, Retina, and the Visual Systems of the Mouse* (Chalupa, L. M., and Williams, R., eds) pp. 721–732, The MIT Press, Cambridge, MA
54. Zhou, J., Jang, Y. P., Kim, S. R., and Sparrow, J. R. (2006) Complement activation by photooxidation products of A2E, a lipofuscin constituent of the retinal pigment epithelium. *Proc. Natl. Acad. Sci. U.S.A.* **103,** 16182–16187
55. Maeda, A., Maeda, T., Golczak, M., and Palczewski, K. (2008) Retinopathy in mice induced by disrupted all-trans-retinal clearance. *J. Biol. Chem.* **283,** 26684–26693
56. Vogel, R., Slakter, J., and McLeod, K. (2009) A phase II, double-masked, placebo-controlled, dose-comparison study of the safety and efficacy of fenretinide in the treatment of geographic atrophy in subjects with age-related macular degeneration: baseline lesion size, characteristics, and preliminary progression data. *Invest. Ophthalmol. Vis. Sci.* **50,** E-abstract 4919
57. Pugliese, G., Pricci, F., Iacobini, C., Leto, G., Amadio, L., Barsotti, P., Frigeri, L., Hsu, D. K., Vlassara, H., Liu, F. T., and Di Mario, U. (2001) Accelerated diabetic glomerulopathy in galectin-3/AGE receptor 3 knockout mice. *FASEB J.* **15,** 2471–2479
58. Yamada, Y., Ishibashi, K., Ishibashi, K., Bhutto, I. A., Tian, J., Lutty, G. A., and Handa, J. T. (2006) The expression of advanced glycation endproduct receptors in rpe cells associated with basal deposits in human maculas. *Exp. Eye Res.* **82,** 840–848
59. Handa, J. T., Verzijl, N., Matsunaga, H., Aotaki-Keen, A., Lutty, G. A., te Koppele, J. M., Miyata, T., and Hjelmeland, L. M. (1999) Increase in the advanced glycation end product pentosidine in Bruch's membrane with age. *Invest. Ophthalmol. Vis. Sci.* **40,** 775–779